



Cite this: *Photochem. Photobiol. Sci.*, 2016, **15**, 1318

Peptide-substituted phthalocyanine photosensitizers: design, synthesis, photophysicochemical and photobiological studies†

Meltem Göksel,^{a,b} Mahmut Durmuş^b and Devrim Atilla^{*b}

A series of phthalocyanine-peptide-quencher conjugates (**6–9**) were synthesized as photosensitizers for photodynamic therapy in cancer treatment. The photophysical, photochemical and photobiological properties of these activatable molecular beacons were also investigated in this study. For this purpose, the fluorescence, singlet oxygen and photodegradation quantum yields and fluorescence lifetime values of the compounds were determined in DMSO solutions. The phototoxicity and cytotoxicity of the systems were studied against the cervical cancer cell line named HeLa for an evaluation of their suitability for photodynamic therapy. The results showed that a maximum of 80% of HeLa cells were killed following light irradiation with photodynamic efficiency. All of the results showed that the novel activatable molecular beacons could be suitable candidates for cancer treatment *via* PDT technique.

Received 30th June 2016,
Accepted 9th September 2016

DOI: 10.1039/c6pp00231e

www.rsc.org/pps

1. Introduction

Phthalocyanine-based compounds play a central role as photosensitizing agents for photodynamic therapy (PDT) of cancer *via* sensitization of tumor tissue to destruction by light. PDT is being relied on to provide improved approaches to targeting treatment. As tumors are developing, they pass through many stages that require the action of proteases. Many tumors overexpress the proteolytic enzymes. Studies have shown that there is a correlation occurs between cancer and the overexpressed proteases.^{1–3} Matrix metalloproteinases (MMPs) play a major role in cell proliferation, migration, angiogenesis and apoptosis.^{4–6} These enzymes are a family of zinc-dependent endopeptidases and overexpression of MMPs promotes the spread of cancer *via* degradation of the extracellular matrix.^{7,8} It is believed that MMPs play key roles in invasive cancer and metastasis because they degrade the extracellular matrix and thus allow malignant cells to cross the basement membrane. MMP expression is upregulated in many types of human cancers and it is associated with an aggressive tumor.^{5,6,9} These enzymes regulate a variety of physiological processes and signaling events and thus they take key roles in the mole-

cular communication between tumor and stroma that regulate cellular function and contribute to tumor progression. MMPs are the most important family of proteinases associated with tumorigenesis.¹⁰

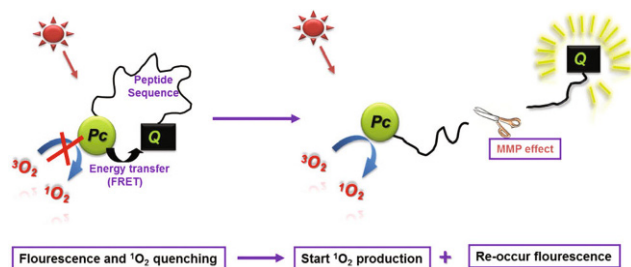
Recently, the number of possible applications of molecular conjugates containing a peptide substrate has been increasing due to their disease-related target enzyme behavior.¹¹ Several activatable peptide-linked conjugates that simply contain either fluorophore or quencher were studied in the literature.¹¹ The peptide linkers in these conjugates are useful to visualize protease activities.^{12–22} Peptide-based conjugates can be detected in their targets *via* restoring fluorescence. These conjugates bear a photosensitizer and a quencher connected with a protease-specific peptide spacer and this system is quenched in the native state because of energy transfer between the photosensitizer and the quencher units. These conjugates become highly fluorescent after proteolysis of the peptide spacer (*via* matrix metalloproteinase cleavage) by the target enzymes which is useful for imaging of the tumor area. On the other hand, the photodynamic activities of these conjugates also increase due to high singlet oxygen generation by the phthalocyanine unit after proteolysis of the peptide spacer (Scheme 1).

Generally, the quencher efficiency of these systems depends on the type of the quenchers. Different types of quenchers can be used for the quenching mechanism. The first strategy relies on a self-quenching mechanism, in which the donor and acceptor groups are on the same or similar fluorophore molecules. These conjugates can be obtained through less complicated synthesis procedures, but generally they exhibit less fluo-

^aKocaeli University, Kosekoy Vocational School, P.O. Box 141, Kartepe, 41135 Kocaeli, Turkey

^bGebze Technical University, Department of Chemistry, PO Box 141, Gebze, 41400 Kocaeli, Turkey. E-mail: datilla@gtu.edu.tr

†Electronic supplementary information (ESI) available. See DOI: 10.1039/c6pp00231e



Scheme 1 Schematic illustration of activatable conjugates. Pc: phthalocyanine as a photosensitizer, Q: quencher, MMP: matrix metalloproteinase.

rescent quenching activity. The second strategy is to use an acceptor molecule which is distinct from the donor, matching the donor fluorophore with the most efficient quencher. This strategy offers the advantage of high quenching efficiency, but increases the complexity of the synthetic process. Activatable peptide-based conjugates consist of a photosensitizer and a quencher attached to opposite ends of a peptide linker.^{23,24}

Activatable photosensitizers produce singlet oxygen at low quantities, so they cause fewer side effects in normal cells which contain a small amount of MMPs due to high energy transfer between photosensitizer and quencher groups in normal cells. High singlet oxygen generation occurs *via* metalloprotease activation by quenched activatable photosensitizers in tumor cells that contain excessive amount of MMPs.

On the other hand, interest in fluorescence-based and other optical imaging techniques for clinical oncology has increased within the past decade. The use of cyanine dyes as contrast agents for *in vivo* optical detection of tumors has been reported by several groups.^{25–28} The targeting of cyanine dyes to tumors was first achieved by using monoclonal antibodies that specifically bind to receptors on tumor cells.^{25,26} Recently, Weissleder *et al.* introduced a new targeting concept for tumor

detection by developing protease-activated near-infrared fluorescent conjugates.²⁸ Many tumors contain overexpressed receptors or other enzymes. The approach of targeting tumors by receptor-avid peptides could potentially be adapted to optical diagnostics when the radiolabel is replaced by a fluorescent dye because fluorescence detection is highly sensitive and can detect 10^{-15} M quantities of fluorescent dyes.²⁹

In the present study, the peptide-based activatable phthalocyanine photosensitizers bearing a polyoxoethylene group were prepared for the first time (Scheme 2).

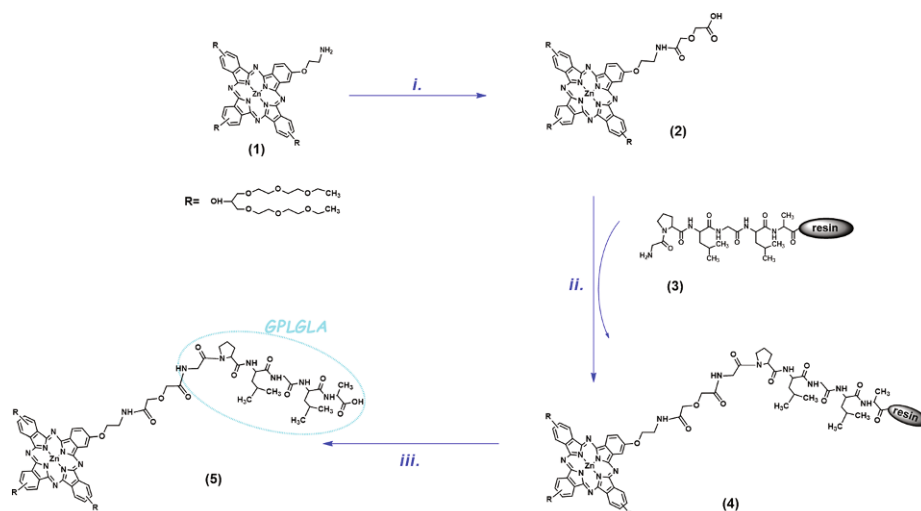
These conjugates consisted of three parts and they showed multiple functions. The first part was an asymmetric zinc(II) phthalocyanine (Pc) used as a photosensitizer, the second part was a peptide sequence which was specific for MMPs and the last part was a quencher compound. One of 2-aminopyrene (Q₁), 1-aminoquinoline (Q₂), atto 680@ (Q₃) or asymmetric mono amino-functionalized zinc(II)Pc (Q₄) was used as quencher. These quencher groups with different absorption wavelengths were selected to compare their quenching efficiencies in the studied conjugates (Fig. 1).

The photophysical and photochemical properties of these conjugates (6–9) such as fluorescence quantum yield, lifetimes, singlet oxygen generation ability and photostability were investigated to determine of their suitability for PDT applications. In addition, the phototoxicity and cytotoxicity activities of these novel conjugates were tested against human HeLa tumor cells.

2. Experimental section

2.1. Materials

All solvents were reagent-grade quality and obtained from commercial suppliers. 1,3-Diphenylisobenzofuran (DPBF) was obtained from Fluka. Unsubstituted zinc Pc (ZnPc) was used as a standard for photophysical and photochemical measure-



Scheme 2 The route for the synthesis of the peptide conjugated asymmetrical zinc(II) phthalocyanine conjugates. (i) Diglycolic anhydride, DMF; (ii) peptide sequence on resin, HBTU, DIPEA, DMF; (iii) TFA/TIS (95 : 5).

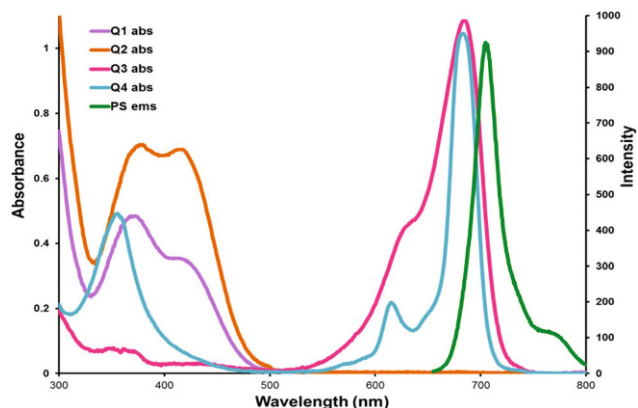


Fig. 1 Electronic absorption spectra of quenchers (Q₁–Q₄) as acceptors and fluorescence emission spectrum of phthalocyanine as donor in DMSO solution.

ments and it was purchased from Aldrich. *N,N*-Diisopropylethylamin (DIPEA) and *O*-(benzotriazol-1-yl)-*N,N,N,N*-tetramethyluronium hexafluorophosphate (HBTU) were purchased from Merck and Sigma-Aldrich, respectively. Wang resins and all of the *N*-R-fmoc-protected amino acids were also purchased from Sigma-Aldrich. All reactions were monitored by thin layer chromatography (TLC) using 0.25 mm silica gel plates (60 F₂₅₄) with UV indicator. Column chromatography was performed on silica gel 60 (0.04–0.063 mm) and preparative thin layer chromatography was also performed on silica gel 60 PF₂₅₄ for the purification of the compounds.

2.2. Equipment

Elemental analyses were obtained from a Thermo Finnigan Flash 1112 Instrument. Infrared spectra were recorded on a Perkin Elmer Spectrum 100 spectrophotometer. Electronic absorption spectra were measured on a Shimadzu 2101 UV-vis spectrophotometer. Fluorescence excitation and emission spectra were recorded on a Varian Eclipse spectrofluorometer using a 1 cm path length cuvette at room temperature. ¹H NMR spectra with tetramethylsilane (TMS) as the internal standard were recorded on a Varian 500 MHz spectrometer. Chemical shifts (δ) were given in ppm relative to DMF-d₇ (8.01 ppm). The mass spectra were obtained on a BRUKER Microflex LT by MALDI (Matrix Assisted Laser Desorption Ionization)-TOF using 2,5-dihydroxybenzoic acid (DHB) as the matrix. The HPLC was performed on an Agilent 1100 series HPLC system (ChemStation software) equipped with a G 1311A pump and G1315B diode array detector monitoring the range 254–900 nm. A reverse phase column Shim-pack ODS (4.0 mm I.D. \times 250 mm L.) (Schimadzu, Japan) was used (HPLC method; gradient solvent mixture 98% of A (0.1% TFA and 99.9% acetonitrile) and 2% of B (methanol) over 20 min; flow rate, 5.0 μ L min⁻¹).

2.3. Photophysical and photochemical parameters

The photophysical and photochemical parameters and used formulas were supplied as ESI.†

2.4. Synthesis

Asymmetrically mono-amine functionalized Zn(II)Pc (**1**) was synthesized and purified according to our previous study.³⁰

2.4.1. Monocarboxy functionalized asymmetric Zn(II)Pc (2). 50 mg, (0.031 mmol) mono-amine functionalized Zn(II)Pc (**1**) in 1 mL DMF was added to 7.2 mg (0.062 mmol) diglycolic anhydride and this mixture was stirred for 48 hours at room temperature. The resulting mixture was extracted by liquid-liquid extraction with ethyl acetate and water. The ethyl acetate phase was dried using anhydrous Na₂SO₄ and solvent was removed under reduced pressure. The purity of the product was checked by TLC. The desired product (**2**) was dried under vacuum. Yield: 45 mg (90%). FT-IR (ν_{\max} /cm⁻¹): 3438 (OH), 3077 (aromatic-CH), 2922–2857 (aliphatic-CH), 1721 (C=O), 1607 (C=C), 1487 (NH), 1392 (aliphatic-CH), 1089 (C–O–C) and 1045 ([C–(C=O)–O–(C=O)–C]). UV-vis (DMSO): λ_{\max} nm (log ϵ) 358 (4.61), 615 (4.20), 685 (4.71). ¹H NMR (DMF-d₇): δ = 0.87–1.03 (m, 18H, CH₃), 3.26–3.35 (m, 24H, CH₂), 3.36–3.38 (m, 2H, CH₂N), 3.47–3.56 (m, 24H, CH₂), 3.59–3.74 (m, 24H, CH₂), 3.77–3.87 (br, 3H, CH), 3.90–3.97 (br, 6H, CH₂O), 7.10–7.81 (m, 8H, ArCH), 7.80–7.82 (br, 2H, OH and NH), 8.94–9.27 (m, 4H, ArCH). Calcd for C₈₃H₁₁₅N₉O₂₆Zn: C%, 57.95; H%, 6.74; N%, 7.33. Found: C%, 58.52; H%, 6.75; N%, 7.68. MS (MALDI-TOF) *m/z*: Calc.: 1720.23; Found: 1721.63 [M + H]⁺.

2.4.2. Peptide sequence (3). The MMP-cleavable peptide sequence GPLGLA-Wang resin (**3**)³¹ was prepared on a 0.2 mmol scale using the fmoc strategy of solid-phase peptide synthesis (SPPS) with commercially available *N*-R-fmoc-protected amino acids. Wang resin and HBTU/DIPEA were used as a solid support and carboxyl-group activating agents, respectively. A two-fold excess of the fmoc-protected amino acids was coupled to the Wang resin. After the final coupling, the last fmoc group was removed from the peptide-resin using 20% piperidine in *N*-methyl-2-pyrrolidone (NMP). The resin was washed with NMP and dichloromethane for removal of the fmoc group from the mixture.

For the characterization of the obtained peptide sequence, a portion of this peptide (**3**) was treated with 95% trifluoroacetic acid (TFA) and 5% triisopropylsilane (TIS) for 1 h at room temperature to cleave the peptide sequence from the Wang resin. After removing the cleaved solid resin by filtration, the filtrate was concentrated and precipitated by adding anhydrous diethyl ether. The white solid product was obtained with good yield (80%). The purity of the obtained peptide was checked by HPLC using acetonitrile containing a 0.1% TFA/MeOH (98 : 2) solvent system and only one peak was observed at 13'94'. FT-IR (ν_{\max} /cm⁻¹): 3304 (OH), 2962–2852 (aliphatic CH), 1643 (C=O), 1539 (C=C), 1455 (NH), 1261 (CH), 1094 (C–O–C), 1024 (CH₂–O). Calcd for C₂₄H₄₂N₆O₇: C%, 54.74; H%, 15.96; N%, 15.96. Found: C%, 54.52; H%, 8.75; N%, 16.08. This peptide was also characterized by MS (MALDI-TOF) *m/z*: Calc.: 526.62; Found: 528.07 [M + 2H]⁺.

2.4.3. Pc-peptide conjugate (5). Monocarboxy functionalized Zn(II)Pc (**2**) (20 mg; 0.012 mmol) was dissolved in 1 mL

DMF. Dicyclohexylcarbodiimide (DCC) (3.6 mg; 0.017 mmol) and *N*-hydroxysuccinimide (NHS) (2 mg; 0.017 mmol) were added to the solution of the Pc (2) and stirred for 10 minutes to activate the carboxyl group. At the end of this time, the peptide sequence (3) (6.1 mg; 0.012 mmol) containing free *N*-terminal amino group swelled in DMF for 1 hour and was added to the reaction mixture. This mixture was also stirred for a further 24 hours at 30 °C. After this time, the reaction mixture was washed with MeOH (2 × 20 mL) and CH₂Cl₂ (2 × 30 mL) to remove unreacted phthalocyanine 2. Phthalocyanine-peptide conjugate (4) was treated with 5 mL of a mixture of TFA/TIS/H₂O (93 : 5 : 2) at room temperature for 4 hours for cleavage of the solid resin. The resin was filtered, washed with TFA (3 × 2 mL), and the filtrates were combined and evaporated under vacuum to give the green targeted compound 5. The obtained conjugate was purified by column chromatography over Bio-Beads® S-X beads using CH₂Cl₂/C₂H₅OH (1 : 1) as eluent. The purity of the conjugate 5 was controlled by reverse-phase HPLC on a Luna C18 semi-preparative column (10 × 250 mm, 5 μm) (Phenomenex, USA) using a solvent system of water and acetonitrile both containing 0.1% TFA, with a stepwise gradient from 50% to 95%. The purity of the Pc-peptide conjugate 5 was found >95%. Yield 5 mg (25%). FT-IR spectrum ($\nu_{\max}/\text{cm}^{-1}$): 3297 (OH), 3069 (aromatic-CH), 2958–2853 (aliphatic-CH), 1648 (C=O), 1545 (C=C), 1457 (NH), 1263 (CH), 1202 (C–N), 1137 (C–O–C). UV-Vis (DMSO): λ_{\max} nm (log ϵ) 360 (4.40), 620 (3.98), 687 (4.71). ¹H NMR (DMF-*d*₇): δ = 0.70–0.79 (m, 33H, CH₃), 1.08–1.19 (bs, 2H, CH), 1.31–1.44 (m, 6H, CH₂), 1.68–1.81 (m, 4H, CH₂), 3.37–3.43/3.53–4.27 (m, 72H, CH₂–O), 3.45–3.52 (m, 8H, CH₂), 4.28–4.33 (m, 4H, CH₂), 4.33–4.38 (m, 7H, CH), 11.66–11.95 (br, 6H, NH), 12.15–12.29/12.37–12.53/12.62–12.91 (m, 12H, ArH), 12.93–13.16 (br, 1H, OH). Calcd for C₁₀₇H₁₅₅N₁₅O₃₂Zn: C%, 57.89; H%, 6.97; N%, 9.38. Found: C%, 57.52; H%, 7.25; N%, 9.68. MS (MALDI-TOF) *m/z*: Calc.: 2228.88; Found: 2269.803 [M + K + 2H]⁺.

2.4.4. Conjugates (6–9). The Pc-peptide conjugate (5) (10 mg; 4.3 μmol) was dissolved in 500 μl of DMF. DCC (1.33 mg; 6.5 μmol) and NHS (0.74 mg; 6.5 μmol) were added to this mixture and then stirred for 2 hours at 50 °C to activate the carboxyl group. After that, the mixture was reacted with a 4.3 μmol quencher such as 6-aminoquinoline (0.62 mg), 1-aminopyrene (0.93 mg), atto-680® (2.24 mg) or asymmetrically mono amino functionalized ZnPc (1) (6.89 mg). After this time, the reaction mixture was precipitated by the addition of 2 mL of hexane and Pc-peptide-quencher conjugates were obtained. The crude products were purified by column chromatography over Bio-Beads® S-X beads using CH₂Cl₂ as eluent. The green solid products were obtained to yield 7.4 mg (74%), 7.22 mg (72%), 7.58 mg (75%), and 7.16 mg (71%) for conjugates 6, 7, 8, and 9, respectively.

Conjugate 6: FT-IR ($\nu_{\max}/\text{cm}^{-1}$): 3311 (NH), 3088 (aromatic-CH), 2965–2878 (aliphatic-CH), 1660–1627 (C=O), 1572–1540 (C=C), 1438 (NH), 1243 (CH), 1088 (C–O–C). UV-vis (DMSO): λ_{\max} nm (log ϵ) 358 (4.25), 620 (3.86), 685 (4.51). ¹H NMR (DMF-*d*₇): δ = 0.82–0.91 (m, 12H, CH₃), 0.98–1.22 (m, 18H,

CH₃), 1.23–1.32 (m, 3H, CH₃), 1.42–1.49 (m, 2H, CH), 2.09–3.13 (m, 10H, CH₂), 3.42–3.92 (m, 72H, CH₂), 4.08–4.29 (m, 12H, CH₂), 4.40–4.53 (m, 4H, CH), 4.55–4.62 (m, 3H, CH), 6.83–7.49 (m, 18H, ArH), 7.93–8.12 (m, 7H, NH). Calcd for C₁₁₆H₁₆₁N₁₇O₃₁Zn: C%, 59.16; H%, 6.89; N%, 10.11. Found: C%, 59.52; H%, 6.75; N%, 10.68. MS (MALDI-TOF) *m/z*: Calc.: 2354.99; Found: 2378.32[M + Na]⁺.

Conjugate 7: FT-IR ($\nu_{\max}/\text{cm}^{-1}$): 3380 (NH), 3051 (aromatic-CH), 2928–2876 (aliphatic-CH), 1664 (C=O), 1609 (C=C), 1493 (NH), 1238 (CH), 1024 (C–O–C). UV-vis (DMSO): λ_{\max} nm (log ϵ) 359 (4.25), 612 (3.86), 686 (4.52). ¹H NMR (DMF-*d*₇): δ = 0.98–1.38 (m, 33H, CH₃), 1.40–1.45 (m, 2H, CH), 1.82–2.03 (m, 6H, CH₂), 2.56–3.40 (m, 4H, CH₂), 3.55–4.12 (m, 72H, CH₂), 4.13–4.45 (m, 12H, CH₂), 4.52–4.72 (m, 7H, CH), 7.59–7.92 (m, 12H, ArH), 7.83–8.01 (m, 7H, NH), 8.04–8.20 (m, 9H, ArH). Calcd for C₁₂₃H₁₆₄N₁₆O₃₁Zn: C%, 60.84; H%, 6.81; N%, 9.23. Found: C%, 60.93; H%, 6.91; N%, 9.55. MS (MALDI-TOF) *m/z*: Calc.: 2428.10; Found: 2452.64 [M + Na + H]⁺.

Conjugate 8: FT-IR ($\nu_{\max}/\text{cm}^{-1}$): 3325 (NH), 3079 (aromatic-CH), 2931–2852 (aliphatic-CH), 1660–1626 (C=O), 1572–1539 (C=C), 1438 (NH), 1244 (CH), 1089 (C–O–C). UV-vis (DMSO): λ_{\max} nm (log ϵ) 354 (4.24), 619 (3.87), 685 (4.56). ¹H NMR (DMF-*d*₇): δ = 0.75–1.03 (m, 15H, CH₃), 1.18–1.39 (m, 18H, CH₃), 1.46–1.54 (m, 9H, CH₃), 1.56–1.62 (m, 2H, CH), 2.16–3.35 (m, 22H, CH₂), 3.39–4.26 (m, 72H, CH₂), 4.29–4.43 (m, 18H, CH₂), 4.45–4.50 (m, 5H, CH), 6.34–6.56 (m, 5H, ArH), 7.03–7.53 (m, 12H, ArH), 7.92–8.33 (b, 7H, NH). Calcd for C₁₃₄H₁₈₅N₁₉O₃₆SZn: C%, 58.84; H%, 6.82; N%, 9.73. Found: C%, 59.02; H%, 6.75; N%, 9.68. MS (MALDI-TOF) *m/z*: Calc.: 2735.46; Found: 2775.23 [M + K + H]⁺.

Conjugate 9. FT-IR ($\nu_{\max}/\text{cm}^{-1}$): 3506 (NH), 3076 (aromatic-CH), 2929–2907 (aliphatic-CH), 1692 (C=O), 1610 (C=C), 1491 (NH), 1398 (CH), 1264 (aromatic-CH), 1101 (C–O–C). UV-vis (DMSO): λ_{\max} nm (log ϵ) 358 (5.09), 615 (4.45), 687 (5.10). ¹H NMR (DMF-*d*₇): δ = 0.90–1.19 (m, 48H, CH₃), 1.32–1.43 (m, 3H, CH₃), 1.48–1.51 (m, 8H, CH), 1.71–1.94 (m, 6H, CH₂), 2.24–3.51 (m, 122H, CH₂), 3.53–4.02 (m, 24H, CH₂), 4.05–4.25 (m, 8H, CH₂), 4.28–4.42 (m, 10H, CH₂), 4.53–4.68 (m, 4H, CH), 6.89–8.20 (m, 31H, ArH/NH). Calcd for C₁₈₆H₂₆₄N₂₄O₅₃Zn₂: C%, 58.56; H%, 6.97; N%, 8.81. Found: C%, 58.02; H%, 6.92; N%, 8.73. MS (MALDI-TOF) *m/z*: Calc.: 3815.00; Found: 3649.81 [M-11CH₃] and 3836.39 [M + Na + H]⁺.

2.5. Biological studies

2.5.1. Cell culture. All tissue culture media and reagents were obtained from PAN Biotech. Human HeLa cells were cultured in DMEM supplemented with 10% fetal bovine serum and antibiotics (penicillin-streptomycin), and incubated at 37 °C in a humidified atmosphere of 5% CO₂ in air. The cells were regularly sub-cultured according to their growth rate.

2.5.2. Light source. The Lumacare Model LC-122 consists of two main parts: a quartz halogen light source (100 W) housing with a control panel and power supply, and a fiber-optic probe (FOP) adapted with filters designed to meet any optical protocol ranging from 380 to 750 nm was used for irradiation of cells. The fiber-optic probes of the LC-122 offer

output power from 10 mW cm^{-2} up to 1 W cm^{-2} at their output tips depending on filter transmission wavelength. For the illumination protocol, a FOP system was used with an activation wavelength of $680 \pm 10 \text{ nm}$. The exposure area was $50 \times 75 \text{ mm}$ and the distance between FOP tip and the cell plate surface was 20 cm . The light power of FOP systems on the exposed area was measured with a power meter that comprises a silicon detector (Ophir). The exposure energy is controlled from the control panel by a timer.

2.5.3. Cytotoxicity studies. The HeLa cells were prepared as described above. Exponentially growing cells were seeded onto 96-well plates at 4000 cells per well and allowed 24 h to attach. Various concentrations of Pc-peptide-quencher conjugates were added to exponentially growing cells and the cells were irradiated with laser irradiation after 24 hour incubation. For dark cytotoxicity experiments, conjugates (6–9) were added to triplicate wells in 0.5; 1; 2; 4; 6; 8 and $10 \mu\text{M}$ final concentration and the cells including these compounds were incubated for 24 hours. The compounds were replaced with fresh medium. And then, cytotoxicity was measured using tetrazolium compound reagent (WST-1, Roche) for the quantification of cell proliferation and cell viability. This is a colorimetric assay and is based on the cleavage of the tetrazolium salt WST-1 by mitochondrial dehydrogenases in proliferating cells.

To each well, $20 \mu\text{L}$ of WST-1 compound was added and the plate was incubated for 4 h before reading. WST-1 tetrazolium compound is metabolized by metabolically active cells into a colored formazan product that can be measured by reading the absorbance at 450 nm with a microplate reader. The average of the triplicate wells for each sample was calculated.

2.5.4. Photo-toxicity studies. For the photo-toxicity experiments, the HeLa cells were prepared as described above and treated with 0.5; 1; 2; 4; 6; 8 and $10 \mu\text{M}$ concentrations of conjugates (6–9) and incubated for 24 hours. After compound loading, the medium was removed and replaced with fresh medium. The cells were exposed to the light from FOP systems with an activation wavelength of 680 nm for determination of photo-toxicity. The total light dose used was 1 and 2 J cm^{-2} . After illumination, the cells were incubated for 24 hours and then 96 well plates were measured by reading the optical density at 450 nm by the Universal Microplate Reader. After incubation, the optical densities were measured using the WST-1 compound as mentioned above.

3. Results and discussion

3.1. Molecular design and synthesis

In the prepared novel molecular beacons, Zn(II)Pc (2) was employed as the photosensitizing agent. The bulky polyoxoethylene glycol chains on the Pc framework were preferred to diminish the aggregation tendency of the systems as well as to enhance the amphiphilicity of the conjugates. The peptide sequence and the Pc ring were linked *via* a peptide bond between the $-\text{CO}_2\text{H}$ group on the Pc core and the $-\text{NH}_2$ group on the peptide sequence. The synthesis route of the Pc conju-

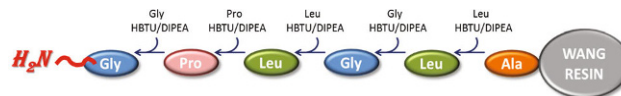


Fig. 2 The synthesis route of peptide sequence *via* SPSS protocol.

gate was given in Scheme 1. The peptide sequence consisting of GPLGLA amino acids was prepared as a substrate to MMPs enzymes overexpressed by cancer cells. The used peptide sequence can be increased by the accumulation of conjugate systems around the cancer cells. The synthesis of the peptide sequence is shown in Fig. 2.

Four different quenchers were attached to this conjugate for preparation of target molecular beacons (6–9). The synthetic routes for the preparation of the molecular beacons were shown in Scheme 3. For the synthesis of designed conjugate systems; firstly, mono-amino functionalized asymmetric Zn(II)Pc (1) was treated with diglycolic anhydride under appropriate conditions²⁵ to obtain the terminal monocarboxy functionalized Zn(II)Pc (2) derivative. NH_2 -GPLGLA-Wang resin (3) was prepared manually, according to the standard 9-fluorenylmethoxycarbonyl (fmoc) solid-phase-peptide synthesis (SPSS) protocol,³² using a Wang resin as a solid phase (Fig. 2) and commercially available fmoc-*N*-protected amino acids. Then the Pc-GPLGLA-Wang resin conjugate (4) was synthesized by the reaction of the Pc 2 which contains a $-\text{CO}_2\text{H}$ group with an N-terminus peptide sequence of 3. This conjugate (4) was cleaved from the Wang resin and Pc-peptide conjugate (5) was obtained. Finally, targeted Pc-peptide-quencher conjugates (6–9) were obtained by the formation of an amide bond between the $-\text{CO}_2\text{H}$ group on the C-terminal alanine of Pc-peptide conjugate 5 and the $-\text{NH}_2$ group on the quenchers (Schemes 2 and 3).

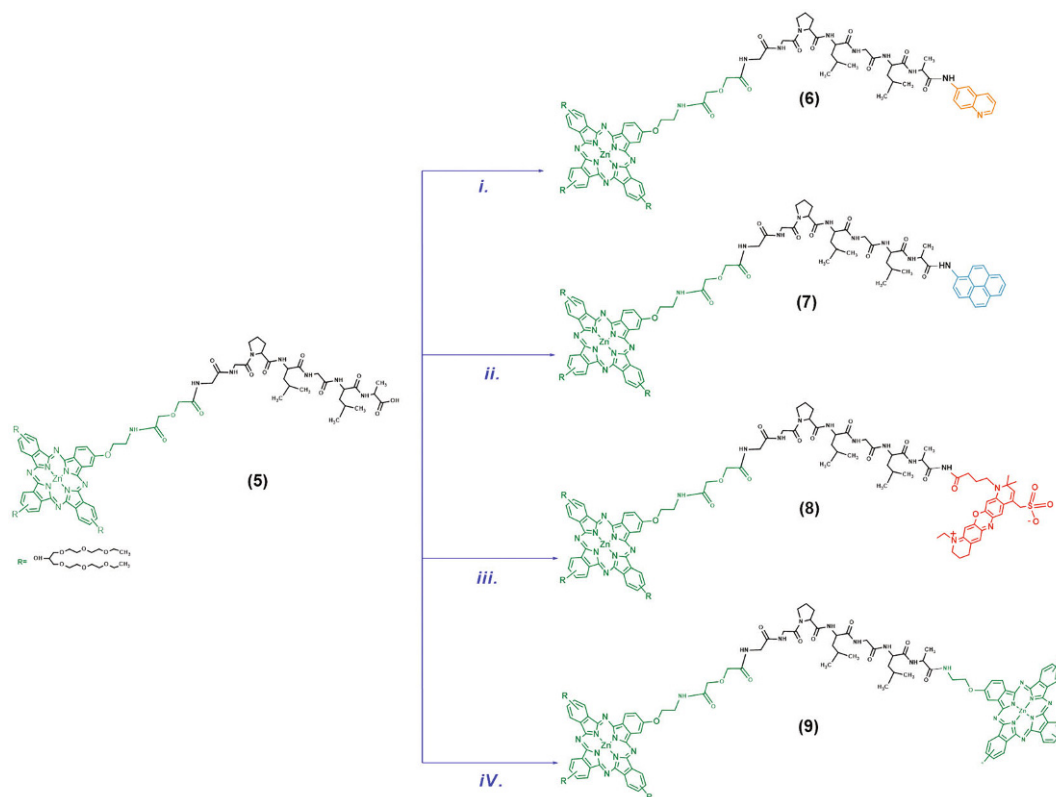
3.2. Characterization

The purity of the synthesized peptide sequence (3) was confirmed by HPLC and it was characterized by MALDI-TOF and FT-IR techniques (Fig. 3).

Newly synthesized mono-carboxy functionalized Zn(II)Pc (2), Pc-peptide conjugate (5), and molecular beacons (6–9) were characterized by different analysis methods, such as ^1H NMR, MALDI-TOF, UV-vis and FT-IR. The purity of conjugate 5 was also confirmed by reverse phase HPLC. The newly synthesized conjugates (6–9) were prepared using different quenchers in order to compare the effects on photophysical, photochemical and photobiological properties of the conjugates. For this purpose, the Pc-peptide conjugate 5 was coupled to four different amino functionalized quenchers.

These quenchers were conjugated to deprotected C-terminal alanine of 5 to obtain conjugates 6, 7, 8, and 9 containing 6-amino-quinoline, 1-amino-pyrene, atto-680® and Pc 1, respectively. The target Pc-peptide-quencher conjugates were characterized by different techniques, such as MALDI-TOF, UV-vis and FT-IR (Fig. 4).

In the FT-IR spectrum of the compound 2, the specific peaks belonging to an anhydride group were observed at 1607



Scheme 3 The route for the synthesis of conjugates 6–9. (i) 6-Aminoquinoline, DCC, NHS, DMF; (ii) 1-Aminopyrene, DCC, NHS, DMF; (iii) Atto 680®, DCC, NHS, DMF; (iv) Pc 1, DCC, NHS, DMF.

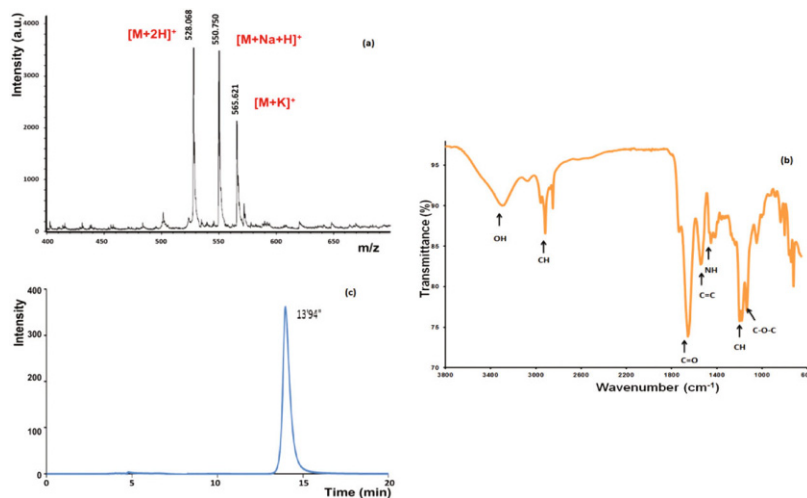


Fig. 3 (a) MALDI-TOF, (b) FT-IR and (c) HPLC spectra of synthesized peptide sequence (3).

and 1721 cm^{-1} after reaction of mono-amino functionalized Pc (1) with diglycolic anhydride. In the FT-IR spectrum of the compound 5, a characteristic peak at 1648 cm^{-1} was related to the peptide sequence.

The FT-IR spectra of the Pc-peptide-quencher conjugates (6, 7, 8, and 9) gave strong evidence for the substitution of different fluorophore groups on the Pc core. After the conju-

gation reaction, the vibration peaks belonging to NH groups, which indicated the formation of an amide bond, appeared in the FT-IR spectra. Zn(II) Pc 6, 7, 8 and 9 showed very similar FT-IR spectra, as expected.

In the $^1\text{H-NMR}$ spectra of the Zn(II)Pc-peptide derivative (5) and its conjugates with quenchers (6, 7, 8, and 9), the aromatic protons were observed between 7.18 and 8.02 ppm for Zn(II)Pc-

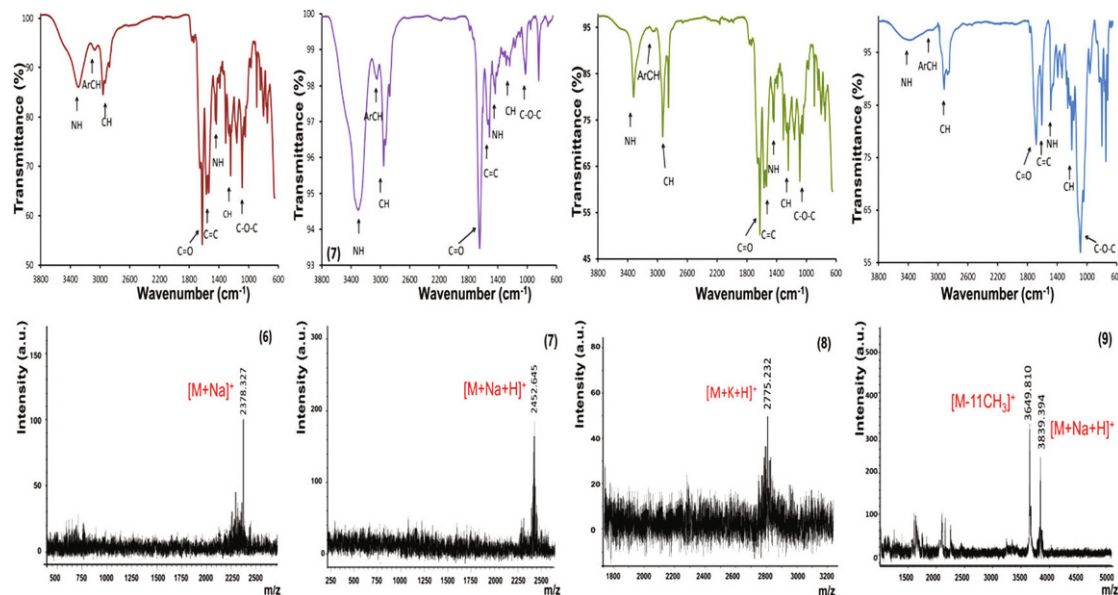


Fig. 4 FT-IR and MALDI-TOF spectra of conjugates 6–9.

peptide derivative (5), 6.83–7.49 ppm for conjugate 6, 7.59–7.92 ppm for conjugate 7, 6.34–6.56 ppm for conjugate 8 and 6.89–8.20 ppm for conjugate 9.

In the MALDI-TOF mass spectra, the molecular ion peaks for Pc-peptide-quencher conjugates (6, 7, 8, and 9) were observed at $m/z = 2270.60 [M + Na]^+$, 2452.64 $[M + Na + H]^+$, 2775.23 $[M + K + H]^+$, and 3839.39 $[M + Na + H]^+$, respectively. These m/z values were consistent with the expected structures of the target conjugates 6, 7, 8 and 9.

3.3. Ground state electronic absorption spectra

The electronic absorption behaviors of terminal $-\text{CO}_2\text{H}$ containing Zn(II)Pc (2), Pc-peptide conjugate (5) and Pc-peptide-quencher conjugates (6–9) were determined by UV-vis spectroscopy. Generally, Pc compounds show two dominant absorption bands at visible and ultraviolet regions in their ground state electronic absorption spectra. These absorption bands are known as Q and B bands. The Q band was observed at around 650–750 nm due to the $\pi \rightarrow \pi^*$ transitions from the highest occupied molecular orbital (HOMO) to the lowest unoccupied molecular orbital (LUMO) of the Pc ring and the B band was observed at around 300–450 nm, arising from deeper π levels \rightarrow LUMO transition.

The electronic absorption spectra of the Pcs showed monomeric behavior in DMSO, evidenced by a single (narrow) Q band in the visible region. The observed spectra were typical for metallated Pc complexes bearing different substituents and central metals.³³ The novel Pcs 2 and 5 showed similar UV-vis spectra and Q bands were observed at 685 nm and 687 nm, respectively. The Q bands were observed at 685 nm, 686 nm, 685 nm and 687 nm for conjugates 6, 7, 8 and 9 in DMSO, respectively. The kind of used quencher did not show any significant effect on the electronic spectra of the studied conju-

gates 6, 7, 8 and 9, because the quenchers were far from the Pc core. The electronic absorption spectra of the studied Zn(II)Pc compound (2), Pc-peptide conjugate (5) and conjugates (6–9) were also measured in different solvents (Fig. 5a is an example for compound 5). All of the studied compounds exhibited similar spectra in toluene, THF, ethanol, DMF, chloroform and DMSO. The spectra showed a single (narrow) Q band, which was evidence of monomeric behavior in all the solvents. The Q bands of the studied Pcs were 10–15 nm red-shifted when compared to unsubstituted ZnPc ($\lambda = 672 \text{ nm}$)³⁴ in DMSO due to the substitution effect. On the other hand, all studied compounds showed a broad band at around 630 nm because of aggregation in water (Fig. 5b is an example for compound 5). The addition of triton X-100 which is a surfactant for reduced aggregation for phthalocyanine compounds to the water solution of these compounds gave a monomeric single narrow Q band due to breaking of the formed aggregates.

3.4. Aggregation studies

In this study, the aggregation behaviors of the Zn(II)Pc 2, Pc-peptide conjugate (5) and Pc-peptide-quencher conjugates (6–9) were also investigated at different concentrations in DMSO (Fig. 6 is an example for compound 8). The Lambert-Beer law was obeyed for all of these compounds at concentrations ranging from 1.2×10^{-5} to 2×10^{-6} M. None of the studied compounds show aggregation at the working concentration range in DMSO.

3.5. Fluorescence spectra

Fluorescence spectra of the Pc derivatives (2, 5, 6–9) were carried out in DMSO. The fluorescence excitation and emission spectra of these compounds were typical of metal Pc complexes in DMSO. The excitation spectra were similar to absorp-

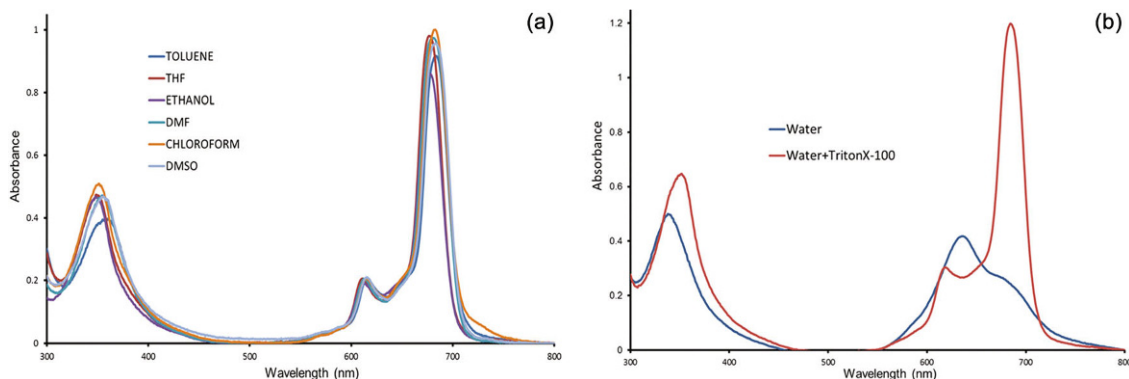


Fig. 5 UV-vis absorption spectra of compound 5 (a) in different solvents and (b) in water and addition of triton X-100 to water solution. Concentration = 1.00×10^{-5} M.

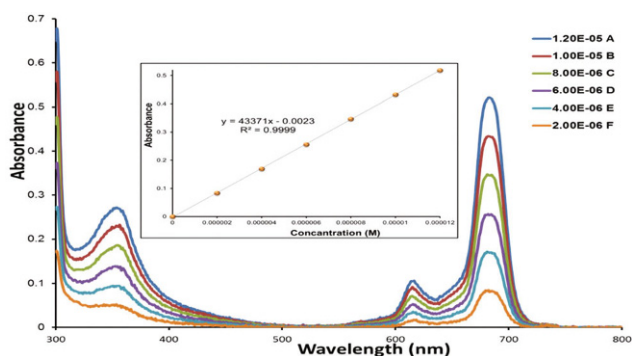


Fig. 6 Absorbance changes of 8 in DMSO at different concentrations: 12×10^{-6} (A), 10×10^{-6} (B), 8×10^{-6} (C), 6×10^{-6} (D), 4×10^{-6} (E), 2×10^{-6} (F) M. (Inset: Plot of absorbance versus concentration.)

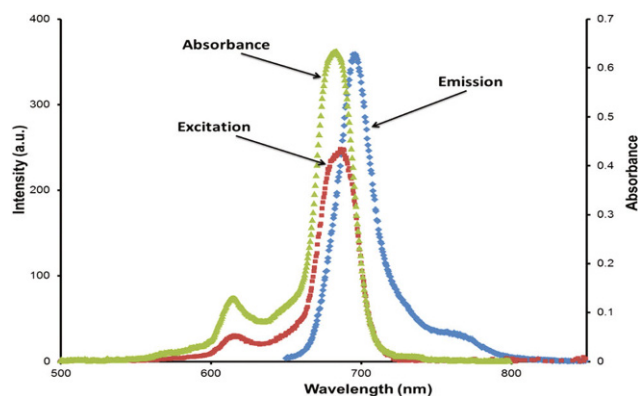


Fig. 7 Absorption, excitation and emission spectra for 7 in DMSO. Excitation wavelength = 650 nm.

tion spectra and both of them were mirror images of the fluorescent spectra for the compounds, suggesting that the molecules did not show any degradation during excitation (Fig. 7 is an example for compound 7). Fluorescence emission maxima were observed at 692 nm for 2, 695 nm for 5, 693 nm for 6, 694 nm for 7, 699 nm for 8 and 696 nm for 9. The Stokes' shifts ($\lambda_{\text{ems}} - \lambda_{\text{exc}}$) ranged from 6 to 14 nm for the studied compounds.

Four different quencher (Q1–Q4) were used to enable the formation of energy transfer in the compounds (6–9). The chemical structures, the absorption spectra of four different quenchers and the emission spectrum of the peptide conjugated Zn(II)Pc (5) are supplied in Table 1 for comparison. In theory, for the formation of non-radiative-energy-transfer (quenching) between quencher and donor, the absorption spectrum of the quencher should overlap the emission spectrum of the donor. However, Lovell *et al.*³⁵ suggested that the spectral overlap is not required for the energy transfer mechanism. It was also proven in our study that spectral overlap is not necessary between the absorption spectrum of a quencher and the emission spectrum of the donor (phthalocyanine).

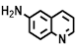
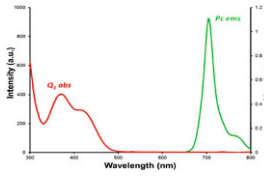
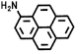
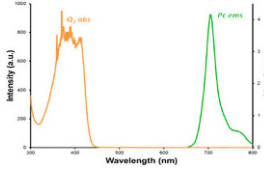
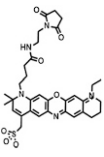
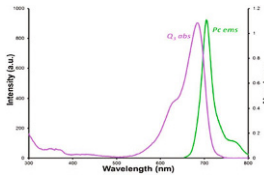
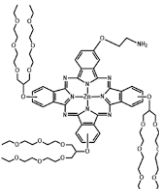
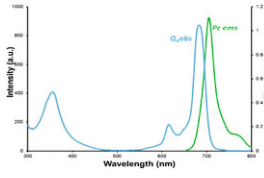
The absorption spectra of the quenchers and emission spectrum of the peptide conjugated Zn(II)Pc (5) are given in

Table 1 and no spectral overlap was shown between compound 5 and 6-aminoquinoline or 1-aminopyrene quenchers. On the other hand, an intense overlap was observed between compound 5 and atto 680® or amino functionalized Pc quenchers. Our results show that overlap is not necessary for efficient quenching in the synthesized novel quenchers. For effective quenching, the energy levels of photosensitizer and quencher should be close.

3.6. Fluorescence quantum yields and lifetimes

Fluorescence occurs when an orbital electron of a photosensitizer relaxes to its ground state by emitting a photon of light after being excited to a higher quantum state. The fluorescence quantum yield (Φ_F) value gives the efficiency of the fluorescence process. This value is defined as the ratio of the number of photons emitted to the number of photons absorbed.³⁶ The Φ_F values of the studied conjugates (6–9) ranged from 0.04 to 0.22 in DMSO (Table 2). These compounds showed very low Φ_F values as a result of energy transfer between phthalocyanine core and quencher, except for conjugate 9. The Φ_F value of the Pc-peptide conjugate (5) decreased by approximately 80% with the substitution of quenchers for

Table 1 The name and structures of used quenchers and overlap graphics between absorption spectra of quenchers and emission spectrum of the peptide conjugated zinc(II) phthalocyanine (5). Concentration = 1.00×10^{-5}

Quencher	Quencher structure	(Q) _{abs} -(PcP) _{ems}
Q ₁ 6-Amino-quinoline λ_{max} : 375		
Q ₂ 1-Amino-pyrene λ_{max} : 390		
Q ₃ Atto-680® λ_{max} : 684		
Q ₄ Phthalocyanine (1) λ_{max} : 686		

conjugates (6, 7 and 8) due to energy transfer between the Pc ring and quenchers. The beacon 9 which was formed by conjugation of two Pc by a peptide sequence showed a higher Φ_F value than other molecular beacons (6–8). This suggested that energy transfer did not occur in this compound because donor and quencher groups were formed from the same Pc ring.

Table 2 Photophysical and photochemical results of studied compounds in DMSO

Compound	Φ_F	τ_F , ns	Φ_Δ	$\Phi_d (\times 10^{-5})$
1 ^a	0.22	2.11	0.71	1.53
2	0.26	3.28	0.70	2.53
5	0.16	4.08	0.46	2.53
6	0.09	1.83	0.14	1.05
7	0.06	1.22	0.16	2.46
8	0.04	1.33	0.17	1.54
9	0.22	1.91	0.32	1.04
Std-ZnPc ^b	0.20	1.22	0.67	2.61

^a Data from ref. 30. ^b Data from ref. 34.

Another proof for the formation of energy transfer between Pc ring and quencher molecules was the reduction in the fluorescence lifetime (τ_F) value of peptide conjugated Zn(II)Pc compound (5) in DMSO after substitution of the different quenchers (Table 2).

3.7. Singlet oxygen quantum yields

Singlet oxygen is formed from a bimolecular interaction between the triplet state of a photosensitizer and ground state (triplet) molecular oxygen. The amount of formed singlet oxygen is described as the singlet oxygen quantum yield (Φ_Δ). The magnitude of singlet oxygen generation depends on the lifetime as well as the energy of the photosensitizer molecules in the triplet state. There is a necessity for high efficiency of energy transfer between the excited triplet state of the photosensitizer and ground state of oxygen to generate large amounts of singlet oxygen for photochemical reactions.³⁶

The singlet oxygen generated by the studied compounds was determined using UV-vis spectroscopy. The absorption decays of DPBF, which is a singlet oxygen scavenger, during light irradiation using a photochemical set-up³⁶ were monitored at 417 nm (Fig. 8 is an example for 9 in DMSO).

The Q band intensities of studied Zn(II)Pcs did not exhibit any changes during the light irradiation for singlet oxygen studies, supporting the theory that these compounds were not degraded during singlet oxygen measurements (Fig. 8 is an example for compound 9).

Table 2 shows that the singlet oxygen quantum yield values of conjugates (6–9) were found to be lower than those of the starting Pc compounds (1–3) in DMSO due to energy transfer from the Pc ring to quencher molecules instead of molecular oxygen.

3.8. Photodegradation studies

Photodegradation studies are often conducted to establish the stability of phthalocyanine molecules on exposure to intense light and hence to determine their efficacy for application in various fields. Photodegradation is a process where a molecule

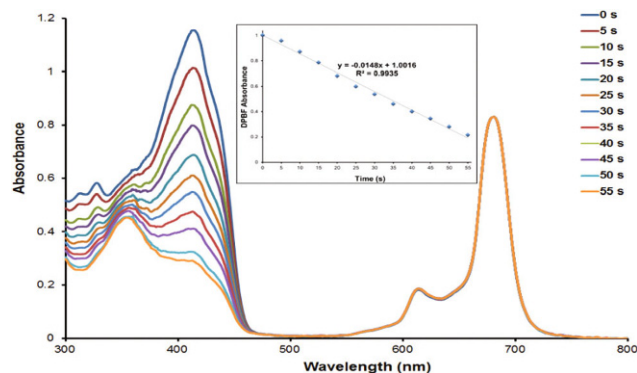


Fig. 8 Absorbance changes during the determination of singlet oxygen quantum yield. This determination was for conjugate 9 in DMSO at a concentration of 1.0×10^{-5} M. (Inset: Plot of DPBF absorbance versus irradiation time.)

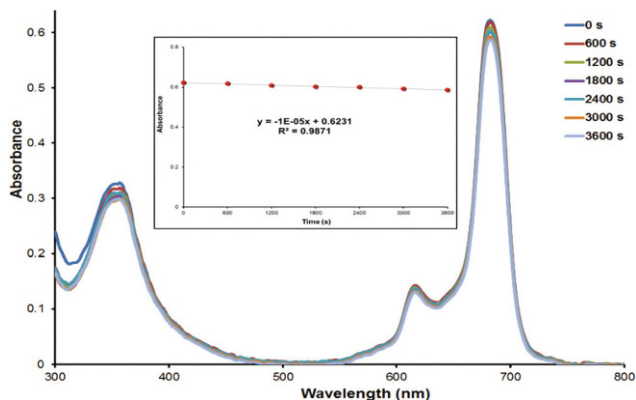


Fig. 9 Absorbance changes during the photodegradation study of **6** in DMSO showing the decreasing of the Q and B bands at 10 minutes intervals (inset: Plot of Q band absorbance versus time).

is degraded under light irradiation. It can be used to determine the stability of molecules and this is especially important for those molecules intended for use as photocatalysts.³⁶

The stabilities of newly synthesized carboxy-functionalized Zn(II)Pc (**2**), Pc-peptide conjugated derivative (**5**) and molecular

beacons (**6–9**) were determined in DMSO by monitoring a decrease in the intensity of the Q-band with increasing time under light irradiation (Fig. 9 for compound **6** is an example). The photodegradation quantum yield (Φ_d) values for the studied compounds (**1–9**) are listed in Table 2. The Φ_d values of the studied Pc (**1–9**) are in the order of 10^{-5} and similar with Pc derivatives bearing different metals in the cavity and substituents on the Pc ring are given in the literature.³⁷ The Φ_d values were reduced when the Pc-peptide conjugate was attached with quenchers, suggesting that the substitution of quenchers increased the stability of the studied Pcs.

3.9. Cell studies

The survival of HeLa cells following illumination with 1 J cm^{-2} (data not shown) and 2 J cm^{-2} of $680 \text{ nm} (\pm 10 \text{ nm})$ (Fig. 10) light after uptake of the Pc **5** and conjugates **6–9** were tested for determination of PDT activity of these photosensitizers in *in vitro* medium. The cell survival percentages of the studied photosensitizers were given in Table 3. Cell survival appears to be dose-dependent and no dark toxicity was observed for any of the photosensitizers. These photosensitizers showed approximately 20% cell survival at a concentration of $10 \text{ } \mu\text{M}$

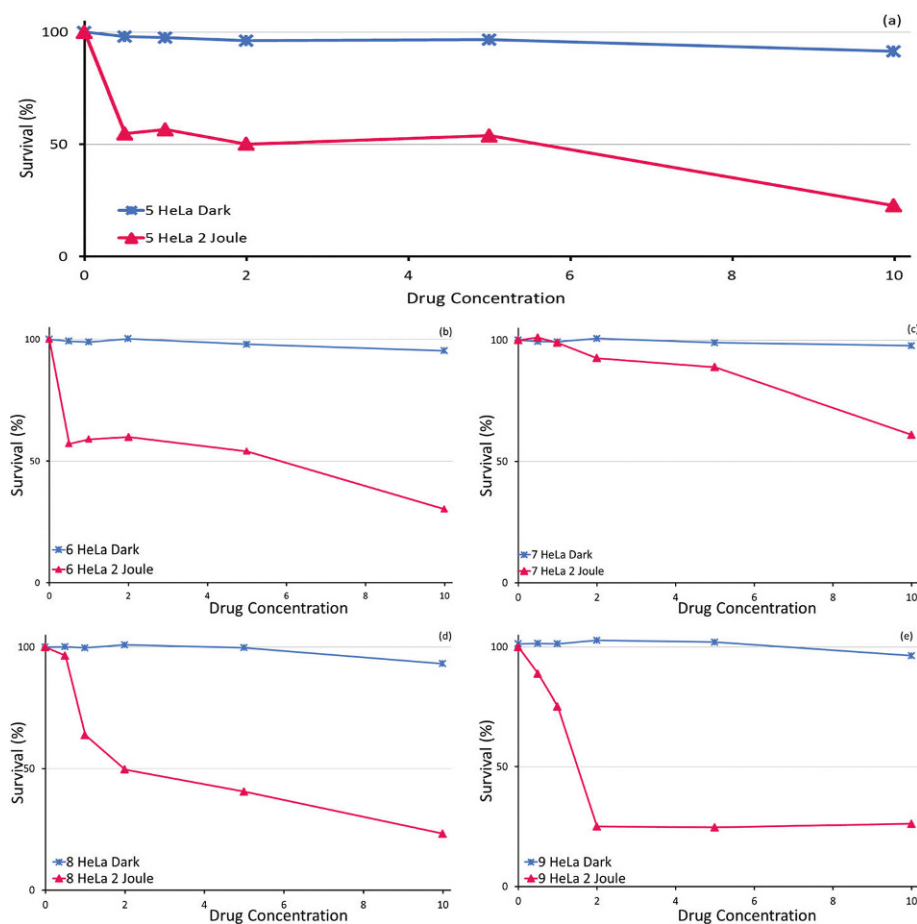


Fig. 10 Survival of HeLa cells following illumination with 2 J cm^{-2} of $680 \text{ nm} (\pm 10 \text{ nm})$ light after 24 h with various concentration of Pc photosensitizers (a) **5**, (b) **6**, (c) **7**, (d) **8** and (e) **9** administration. Each data represents the mean \pm SD of three experiments.

Table 3 Percentage of HeLa cells survival following illumination with 2 J cm^{-2} at 680 nm ($\pm 10 \text{ nm}$) light after 24 hours incubation with various concentrations of photosensitizer molecules (**5**, **6**, **7**, **8**, and **9**)

Concentration (μM)	Pc-Photosensitizers (survival, %)				
	5	6	7	8	9
0.5	54	57	101	96	88
1	56	58	98	63	75
2	50	59	92	49	24
5	53	53	88	40	24
10	22	30	61	23	26

after 2 J cm^{-2} irradiation, except for conjugate **7** which showed approximately 60% cell survival in the same conditions.

After treatment of 2 J cm^{-2} irradiation with $2 \mu\text{M}$, the cell survivals were found to decrease by approximately 50% for **5**, **6** and **8** (Table 3). The cell survival was found to be 92% after treatment of 2 J cm^{-2} irradiation with $2 \mu\text{M}$ for conjugate **7**. This conjugate showed very limited PDT activity, suggesting

that the conjugation of 1-amino-pyren to Pc-peptide derivative reduced photosensitizer efficiency. The conjugate **9** showed most activity among the studied photosensitizers, with 24% cell survival at 2 J cm^{-2} light irradiation against HeLa cells. As a result of the two-fold photosensitizer concentration in the cell culture high cytotoxicity was shown with conjugate **9**.

On the other hand, the studied photosensitizers were added to exponentially growing cells and then incubated 24 hours for determination of fluorescence behavior of these photosensitizers. After this time, fluorescence re-occurs in the cell culture supernatant because of MMPs activity in HeLa cells. As a result the intramolecular energy transfer is reduced by the photoactivity of the molecules. Fig. 11 shows the increase in fluorescence intensities of studied photosensitizers (**5–9**) after MMP activity. These results show that the studied novel conjugate systems cleave on the peptide sequence in the HeLa cells and fluorescence emissions of quenchers re-occur due to the formation of free quenchers in this cell medium.

The obtained photophysical and photochemical data such as singlet oxygen quantum yields (Φ_{Δ}), fluorescence quantum yields (Φ_F) and fluorescence lifetime (τ_F) were compared as % values in DMSO (Fig. 12). As shown in this figure, there was quite an effective decrease in these values after conjugation of the quencher to the Pc ring. These results proved that energy transfer was occurring between the Pc core and the quencher.

4. Conclusion

In this study, the synthesis of the novel Pc-peptide-quencher molecular beacons (**6–9**) was successfully achieved. These conjugates were characterized by standard methods including UV-vis, ^1H NMR, FT-IR, MALDI-TOF mass and elemental analysis as well. The photophysical and photochemical properties such as fluorescence quantum yields, lifetimes and singlet oxygen quantum yields of these conjugates were investigated in DMSO. In addition, the photodynamic activities of these conjugates (**6–9**) were tested against human HeLa cells. All these properties of the novel conjugates were compared to the starting Pc (**5**). These conjugates were PDT inactive until they reached the cancerous cells according to their photophysical and photochemical properties. It may be concluded that energy transfer happened between the Pc ring and the fluorophore group. These conjugates could be active in the cancer cells due to cleavage of the peptide sequence by MMP enzymes in cancer cells. These MMP enzymes are secreted at a limited level in normal cells.

According to the results, intramolecular energy transfer occurred in synthesized novel conjugates (**6–9**) and they could be passive until they reach the target cancer tissue. Thus the synthesized novel conjugates may serve as activatable photosensitizers. They could be useful because they are non-toxic to healthy tissue and they could exhibit good photodynamic activity in cancer cells.

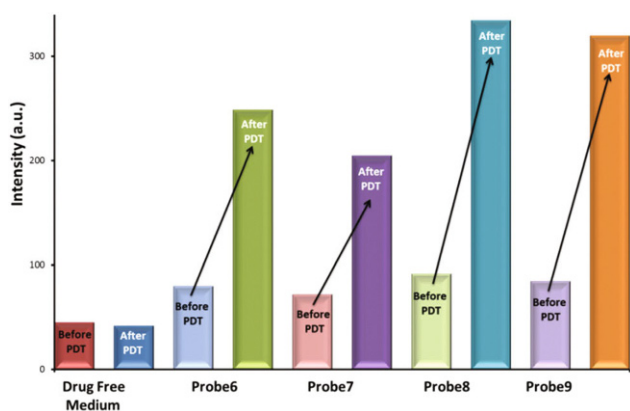


Fig. 11 Fluorescence intensity of the cell culture supernatant, after treatment of conjugates (**6–9**) treatment.

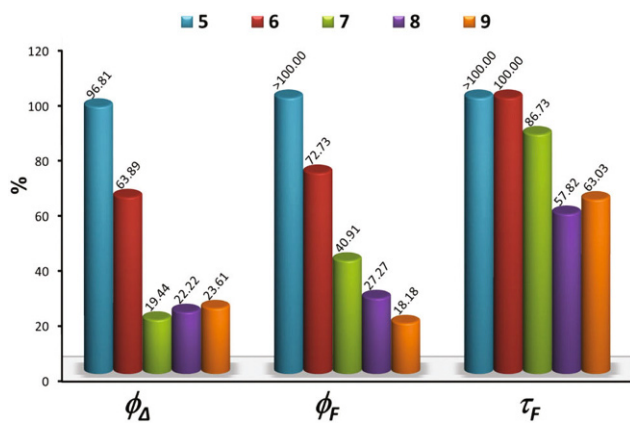


Fig. 12 The comparison of the singlet oxygen quantum yield (Φ_{Δ}), fluorescence quantum yield (Φ_F) and fluorescence lifetime (τ_F) data as % values of novel conjugates (**6–9**) with starting Pc (**5**) in DMSO.

References

- 1 M. R. Detty, S. L. Gibson and S. J. Wagner, *J. Med. Chem.*, 2004, **47**, 3897–3915.
- 2 B. Turk, *Nat. Rev.*, 2006, **5**, 785–799.
- 3 B. Law and C. Tung, *Bioconjugate Chem.*, 2009, **20**, 1683–1695.
- 4 M. Cicek and M. J. Oursler, *Cancer Metastasis Rev.*, 2006, **25**, 635–644.
- 5 R. L. Scherer, J. O. Mc Intyre and L. M. Matrisian, *Cancer Metastasis Rev.*, 2008, **27**, 679–690.
- 6 T. W. Liu, J. Chen and G. Zheng, *Amino Acids*, 2011, **41**(2), 1123–1134.
- 7 C. E. Brinckerhoff and L. M. Matrisian, *Nat. Rev. Mol. Cell Biol.*, 2002, **3**, 207–214.
- 8 T. A. Guise, *Genes Dev.*, 2009, **23**, 2117–2123.
- 9 M. Ii, H. Yamamoto, Y. Adachi, Y. Maruyama and Y. Shinomura, *Exp. Biol. Med.*, 2006, **231**, 20–27.
- 10 K. Kessenbrock, V. Plaks and Z. Werb, *Cell*, 2010, **141**, 52–67.
- 11 C. H. Tung, *Biopolymers*, 2004, **76**, 391–403.
- 12 T. Jiang, E. S. Olson, Q. T. Nguyen, M. Roy, P. A. Jennings and R. Y. Tsien, *Proc. Natl. Acad. Sci. U. S. A.*, 2004, **101**, 17867–17872.
- 13 E. A. Goun, R. Shinde, K. W. Dehnert, A. Adams-Bond, P. A. Wender, C. H. Contag and B. L. Franc, *Bioconjugate Chem.*, 2006, **17**, 787–796.
- 14 G. Blum, S. R. Mullins, K. Keren, M. Fonovic, C. Jedeszko, M. J. Rice, B. F. Sloane and M. Bogyo, *Nat. Chem. Biol.*, 2005, **1**, 203–209.
- 15 D. Kato, K. M. Boatright, A. B. Berger, T. Nazif, G. Blum, C. Ryan, K. A. Chehade, G. S. Salvesen and M. Bogyo, *Nat. Chem. Biol.*, 2005, **1**, 33–38.
- 16 G. Blum, G. von Degenfeld, M. J. Merchant, H. M. Blau and M. Bogyo, *Nat. Chem. Biol.*, 2007, **3**, 668–677.
- 17 M. Verhille, H. Benachour, A. Ibrahim, M. Achard, P. Arnoux, M. Barberi-Heyob, J. C. Andre, X. Allonas, F. Baros, R. Vanderesse and C. Frochot, *Curr. Med. Chem.*, 2012, **19**, 5580–5594.
- 18 M. Verhille, P. Couleaud, R. Vanderesse, D. Brault, M. Barberi-Heyob and C. Frochot, *Curr. Med. Chem.*, 2010, **17**, 3925–3943.
- 19 J. Chen, K. Stefflova, M. J. Niedre, B. C. Wilson, B. Chance, J. D. Glickson and G. Zheng, *J. Am. Chem. Soc.*, 2004, **126** (37), 11450–11451.
- 20 G. Zheng, J. Chen, K. Stefflova, M. Jarvi, H. Li and B. C. Wilson, *Proc. Natl. Acad. Sci. U. S. A.*, 2007, **104**(21), 8989–8994.
- 21 J. Chen, K. Stefflova, M. Warren, J. Bu, B. C. Wilson and G. Zheng, *Proc. SPIE-Int. Soc. Opt. Eng.*, 2007, **6449**, 1–9, (Genetically Engineered and Optical Probes for Biomedical Applications IV).
- 22 P. Lo, J. Chen, K. Stefflova, M. S. Warren, R. Navab, B. Bandarchi, S. Mullins, M. Tsao, J. D. Cheng and G. Zheng, *J. Med. Chem.*, 2009, **52**(2), 358–368.
- 23 J. F. Lovell, T. W. B. Liu, J. Chen and G. Zheng, *Chem. Rev.*, 2010, **110**, 2839–2857.
- 24 S. Lee, K. Park, K. Kim, K. Choi and I. C. Kwon, *Chem. Commun.*, 2008, 4250–4260.
- 25 B. Ballou, *et al.*, *Cancer Immunol. Immunother.*, 1995, **41**, 257–263.
- 26 K. Licha, *et al.*, *Photochem. Photobiol.*, 2000, **72**, 392–398.
- 27 A. Becker, *et al.*, *Photochem. Photobiol.*, 2000, **72**, 234–241.
- 28 R. Weissleder, C. H. Tung, U. Mahmood and A. Bogdanov Jr., *Nat. Biotechnol.*, 1999, **17**, 375–378.
- 29 A. Becker, C. Hassenius, K. Licha, B. Ebert, U. Sukowski, W. Semmler, B. Wiedenmann and C. Grötzinger, *Nat. Biotechnol.*, 2001, **19**, 327–331.
- 30 M. Göksel, M. Durmuş and D. Atilla, *J. Photochem. Photobiol. A*, 2013, **266**, 37–46.
- 31 M. Sibrian-Vazquez, J. Ortiz, I. V. Nesterova, F. Fernandez-Lazaro, A. Sastre-Santos, S. A. Soper and M. G. H. Vicente, *Bioconjugate Chem.*, 2007, **18**, 410–420.
- 32 R. B. Merrifield, *J. Am. Chem. Soc.*, 1963, **85**(14), 2149–2154.
- 33 M. J. Stillman and T. Nyokong, in *Phthalocyanines: Properties and Applications*, ed. C. C. Leznoff and A. B. P. Lever, VCH Publishers, New York, 1989, vol. 1, ch. 3.
- 34 I. Gürol, M. Durmuş, V. Ahsen and T. Nyokong, *Dalton Trans.*, 2007, **34**, 3782–3791.
- 35 J. F. Lovell, J. Chen, M. T. Jarvi, W. Cao, A. D. Allen, Y. Liu, T. T. Tidwell, B. C. Wilson and G. Zheng, *J. Phys. Chem. B*, 2009, **113**, 3203–3211.
- 36 M. Durmuş, Photochemical and photophysical characterization, in *Photosensitizers in Medicine, Environment, and Security*, ed. T. Nyokong and V. Ahsen, Springer, New York, 2012, pp. 135–267.
- 37 T. Nyokong, *Coord. Chem. Rev.*, 2007, **251**, 1707–1722.